

# A novel adaptive constant power optimal efficiency control strategy for bidirectional DS-LCC wireless charger

Jiabo Yan<sup>1,2</sup>, Mohd Junaidi Abdul Aziz<sup>1</sup>, Nik Rumzi Nik Idris<sup>1</sup>, Mohammad Al Takrouri<sup>1</sup>,  
Tole Sutikno<sup>3,4</sup>

<sup>1</sup>Faculty of Electrical Engineering, Universiti Teknologi Malaysia, Johor, Malaysia

<sup>2</sup>Nanning Engineering Technology Research Center for Power Transmission System of New Energy Vehicle, College of Traffic and Transportation, Nanning University, Nanning, China

<sup>3</sup>Department of Electrical Engineering, Faculty of Industrial Technology, Universitas Ahmad Dahlan, Yogyakarta, Indonesia

<sup>4</sup>Embedded System and Power Electronics Research Group, Yogyakarta, Indonesia

## Article Info

### Article history:

Received Jun 4, 2025

Revised Oct 22, 2025

Accepted Dec 11, 2025

### Keywords:

Constant-power

Double-sided LCC

Inductive power transfer

Optimal efficiency

Wireless power transfer

## ABSTRACT

This paper presents a novel adaptive constant power optimal efficiency control (ACPOEC) strategy that enables efficient constant power (CP) charging in a double-sided inductor-capacitor-capacitor (DS-LCC) wireless charger. The proposed control strategy is built upon triple-phase-shift (TPS) modulation and employs a pre-computed lookup table derived from offline optimization to achieve CP charging with corresponding optimal efficiency. The CP charger with the proposed strategy can eliminate switch-controlled capacitors (SCCs) in the topology. The proposed strategy is validated through simulation studies, achieving an efficiency range of 90.72% to 92.46%, which is also competitive with other advanced CP wireless charging systems. Compared with existing state-of-the-art CP wireless charging techniques, the wireless CP charger with the proposed ACPOEC strategy features a simplified topology, bidirectional power transfer capability, and competitive efficiency performance.

This is an open access article under the [CC BY-SA](#) license.



## Corresponding Author:

Mohd Junaidi Abdul Aziz

Faculty of Electrical Engineering, Universiti Teknologi Malaysia

Balai Cerap UTM, Lengkok Suria, 81310 Skudai, Johor, Malaysia

Email: junaidi@utm.my

## 1. INTRODUCTION

In the domain of battery charging, the traditional constant current (CC) charging method remains the predominant approach [1], [2]. However, CC charging does not fully exploit the available power capacity of the power source and charger. As shown in Figure 1(a), the output power is low when the battery voltage is low. This limitation leads to under utilization of the charger's and power supply's capabilities, extending the overall charging duration.

Compared to CC charging, constant power (CP) charging maintains a consistent power transfer throughout the entire charging process [3], as shown in Figure 1(b). This charging method adjusts the output current through control strategies in response to variations in battery voltage. This CP charging can fully utilize the available power capacity of the equipment, thereby accelerating the charging process and reducing the overall charging time. Moreover, CP charging has been shown to alleviate battery degradation issues [4], [5].

Inductive power transfer (IPT) wireless chargers are widely adopted across various industries, such as consumer electronics [6]–[8], biomedical implants [9]–[11], electric bikes [5], [12], [13], and electric vehicles

(EVs) [4], [14], [15], due to their advantages including inherent safety, low maintenance, and high reliability. To realize CP charging in wireless systems, extensive research has been conducted. A common method is incorporating a DC-DC converter on either the input or output side to regulate voltage or current [16], [17]. However, this additional power conversion stage increases system cost, power losses, and overall complexity.

To avoid using an additional DC-DC conversion stage, several single-stage CP wireless charging solutions have been proposed. For example, single-stage CP wireless chargers utilizing series-series (S-S) compensation networks have been explored in the literature [18]–[20]. However, S-S compensated wireless chargers are prone to generating excessive current under the coupler misalignment condition, thereby requiring supplementary safety protection mechanisms.

To deal with this safety concern in wireless power transfer systems, inductor-capacitor-capacitor (LCC) resonant compensation topologies, such as LCC-series (LCC-S) and double-sided LCC (DS-LCC), have emerged as effective solutions. In [5], an LCC-S compensation network combined with pulse-density modulation (PDM) was employed to achieve CP operation and efficiency optimization. However, this charger lacks bidirectional power transfer capability, limiting its suitability for applications aligned with the Energy Internet paradigm.

The DS-LCC compensation topology not only addresses safety concerns but also supports bidirectional power transfer. Owing to this critical advantage, the DS-LCC topology is widely used in IPT systems and is also adopted by industry standards [21]. However, the traditional DS-LCC wireless charger is a kind of CC charger only. To enable the CP charging function in DS-LCC wireless chargers, author in [22] proposed a DS-LCC charger incorporating two switch-controlled capacitors (SCCs). While this approach successfully achieves CP charging, the dependence on multiple SCCs introduces several drawbacks, including increased component costs and additional power losses.

In the IPT field, a DS-LCC wireless charger employing a triple-phase-shift (TPS) modulation strategy was proposed in [23]. This approach enables zero-voltage switching (ZVS) over a wide operating range without the use of any SCCs, resulting in a simplified circuit structure and high efficiency. However, the system is not capable of achieving CP charging for batteries. This paper proposes a novel adaptive constant power optimal efficiency control (ACPOEC) strategy for a DS-LCC bidirectional wireless charger. The ACPOEC strategy is built upon triple-phase-shift (TPS) modulation and employs a pre-computed lookup table derived from offline optimization to achieve CP charging with corresponding optimal efficiency.

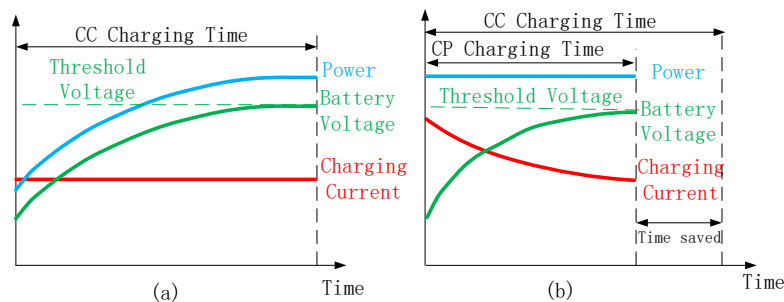


Figure 1. Comparison between (a) CC charging and (b) CP charging

## 2. THE WIRELESS CP CHARGER WITH THE PROPOSED ACPOEC STRATEGY

### 2.1. Charging system structure

The topology of the bidirectional DS-LCC wireless charging system is illustrated in Figure 2. On the primary side, an inverter composed of four MOSFETs ( $S_1$  to  $S_4$ ) is used to generate the AC voltage, while on the secondary side, an active rectifier consisting of four MOSFETs ( $S_5$  to  $S_8$ ) is employed to convert the AC current into DC current. The compensation network includes series inductors  $L_1$  and  $L_2$ , parallel capacitors  $C_1$  and  $C_2$ , series compensation capacitors  $C_p$  and  $C_s$ , and coil self-inductances  $L_p$  and  $L_s$ .

The  $C_O$  is a DC-link capacitor on the secondary side. The input DC voltage and battery voltage are represented by  $V_1$  and  $V_2$ . The inverter's output voltage and current are labeled as  $u_{ab}$  and  $i_{L1}$ , while the rectifier's input voltage and current are denoted by  $u_{cd}$  and  $i_{L2}$ . The mutual inductance between the couplers is indicated as  $M$ , and the coupling coefficient  $k$  is defined by  $k = M/\sqrt{L_p L_s}$ .

The inverter output voltage is denoted as  $u_{ab}$ , and the rectifier input voltage is denoted as  $u_{cd}$ . Variables  $u_p$  and  $u_s$  represent the fundamental components of  $u_{ab}$  and  $u_{cd}$ , respectively. The phase difference between  $u_p$  and  $u_s$  is denoted by  $\delta$ . The duty cycles of  $u_{ab}$  and  $u_{cd}$  are represented by  $D_p$  and  $D_s$ , respectively. To facilitate the analysis and simplify the equations, a phase shift compensation angle  $\Delta\delta$  is defined as  $\Delta\delta = \delta - \frac{\pi}{2}$ .

The optimum phase shift  $\Delta\delta$ , denoted as  $\Delta\delta_{opt}$ , ensuring that all switches in the system work under ZVS, according to [24], is expressed as (1).

$$\Delta\delta_{opt} = -D_S \frac{\pi}{2} + \cos^{-1} \left( \Lambda^{-1} \times \left( -2\pi\omega L_1 L_2 I_{ZVS} + \frac{V_2 L_1}{D_S \frac{\pi}{2} - 8 \sin^2(D_S \frac{\pi}{2})} \right) \right) \quad (1)$$

Where  $\Lambda = 8MV_1 \sin(\frac{\pi}{2} D_p)$ , and  $I_{ZVS}$  is the predefined threshold current required for ZVS, which is used to charge and discharge the MOSFETs' equivalent output capacitance during the dead time. Neglecting losses in the charger, the transferred power can be expressed as (2).

$$P = \frac{M}{\omega L_1 L_2} |\dot{U}_P| |\dot{U}_S| \sin\left(\frac{\pi}{2} + \Delta\delta\right) \quad (2)$$

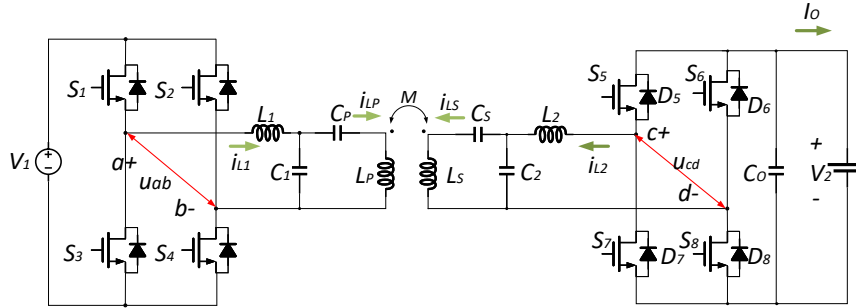


Figure 2. Topology of the bidirectional DS-LCC wireless charger

## 2.2. Coupling coefficient estimation

In the control strategy, the coupling coefficient needs to be estimated to achieve the adaptive control. A coupling coefficient estimation method is developed. In the estimation method, switches  $S_7$  and  $S_8$  are turned on to force  $u_{cd} = 0$ , as illustrated in Figure 3.

Ignoring losses, the coupling coefficient  $k$  can be expressed as a function of  $I_{L2}$  as (3).

$$I_{L2} = \frac{k \sqrt{L_p L_s} \cdot U_{ab}}{\omega L_1 L_2} \quad (3)$$

Obviously,  $I_{L2}$  is proportional to the coupling coefficient  $k$ . Therefore, if we want to estimate the coupling coefficient  $k$ , we can measure the current  $I_{L2}$ . To improve accuracy,  $I_{L2}$  can be experimentally measured for discrete values of  $k$ , allowing the creation of a lookup table that defines the relationship between  $I_{L2}$  and  $k$ . This lookup table can then be utilized by the controller to estimate  $k$  based on  $I_{L2}$ , as illustrated in Figure 3.

$I_{L2}$  can be measured at discrete values of  $k$  experimentally, and a lookup table that maps the relationship between  $I_{L2}$  and  $k$  can be built. The controller can subsequently use this lookup table to estimate  $k$  based on the measured  $I_{L2}$ , as illustrated in Figure 3.

## 2.3. ACPOEC strategy for CP charging

The ACPOEC strategy implemented in the proposed CP charger is illustrated in Figure 4. In this strategy, the controller on the secondary side acquires the battery voltage  $V_2$  and retrieves the optimal control variables under this  $V_2$  in the lookup table. This lookup table is produced by the offline optimization method shown in Figure 5, which is explained in the next section. The optimal variables  $D_{s\_opt}$  and  $\Delta\delta_{opt}$  are sent to pulse generators in the secondary side controller as a parameter. In the meantime, the secondary controller sent optimal duty cycle  $D_{p\_opt}$  to the primary controller by wireless communication. The optimum variable can make the wireless charger achieve CP charging with corresponding optimum efficiency.

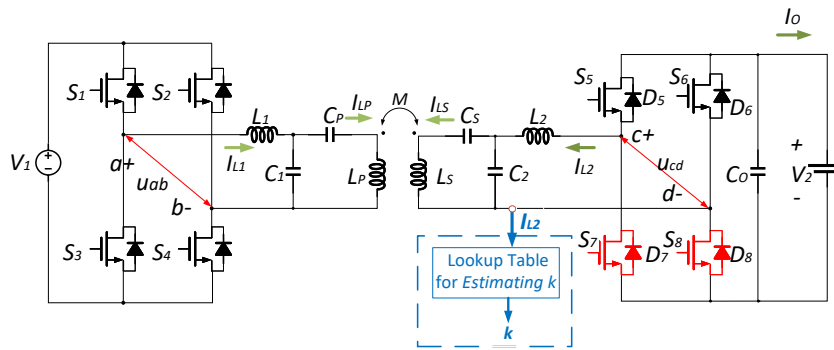


Figure 3. Diagram of coupling coefficient estimation

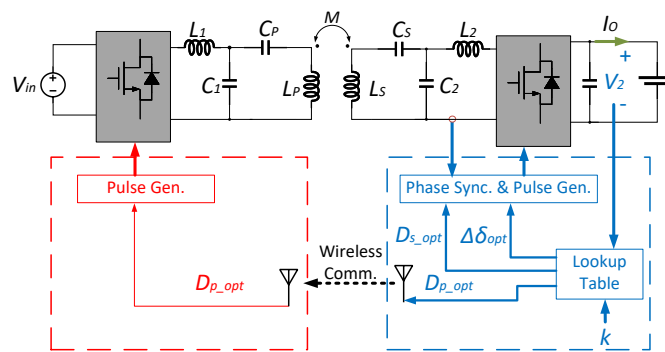


Figure 4. Proposed control strategy

#### 2.4. Offline optimization approach

The optimum variables in the lookup table are generated by the offline optimization approach. The goal of the optimization is to pick the optimal control variables that maximize efficiency while ensuring constant power output across a range of battery voltages. To get maximum efficiency, loss model is built in this section.

The total power loss can be separated into losses in the inverter, losses in the resonant network, and losses in the rectifier. Inverter's losses include conduction losses and switching losses. Since all switches achieve ZVS, the switching losses are very tiny and can be omitted in the overall power loss optimization [23]. The losses in the inverter can be expressed as (4).

$$P_{inv} = 2R_{ON}I_{L1}^2 \quad (4)$$

Similarly, the losses from the rectifier are expressed as (5).

$$P_{rec} = 2R_{ON}I_{L2}^2 \quad (5)$$

Losses in the resonant circuit are expressed as (6).

$$P_{res} = I_p^2 R_{L1} + I_s^2 R_{L2} + I_{LP}^2 (R_{LP} + R_{CP}) + I_{LS}^2 (R_{LS} + R_{CS}) + I_{C1}^2 R_{C1} + I_{C2}^2 R_{C2} \quad (6)$$

Here,  $R_{CP}$ ,  $R_{CS}$ ,  $R_{C1}$ , and  $R_{C2}$  refer to the equivalent series resistances (ESRs) of the capacitors  $C_P$ ,  $C_S$ ,  $C_1$ , and  $C_2$ , respectively.

Thereby, the total losses in the charger can be expressed as (7).

$$P_l = P_{inv} + P_{rec} + P_{res} \quad (7)$$

With the loss model built above, the offline optimization method is proposed, as illustrated in Figure 5. The process involves the following steps: (i) Initialization: Provide system parameters, like input voltage  $V_1$ , the range of coupling coefficients  $k_{min}$  and  $k_{max}$ , and the range of battery voltages  $V_{2min}$  and  $V_{2max}$ , the reference

power  $P_{ref}$ ; (ii) Discretizing coupling coefficient  $k$ : Sample the coupling coefficient  $k$  over its predefined range using an appropriate step size; (iii) Discretizing battery voltage  $V_2$ : Sample the battery voltage  $V_2$  over its predefined range with an appropriate step size; (iv) Control variable searching for CP charging: If the calculated power matches the reference power  $P_{ref}$  within a specified tolerance  $e$ , the corresponding control variables are retained. If both  $D_P$  and  $D_S$  already reach the maximum value of 1 and the transferred power still does not meet  $P_{ref}$ , the combination  $D_P = D_S = 1$  and the associated  $\Delta\delta_{opt}$  are preserved to track the maximum deliverable power with optimal efficiency.

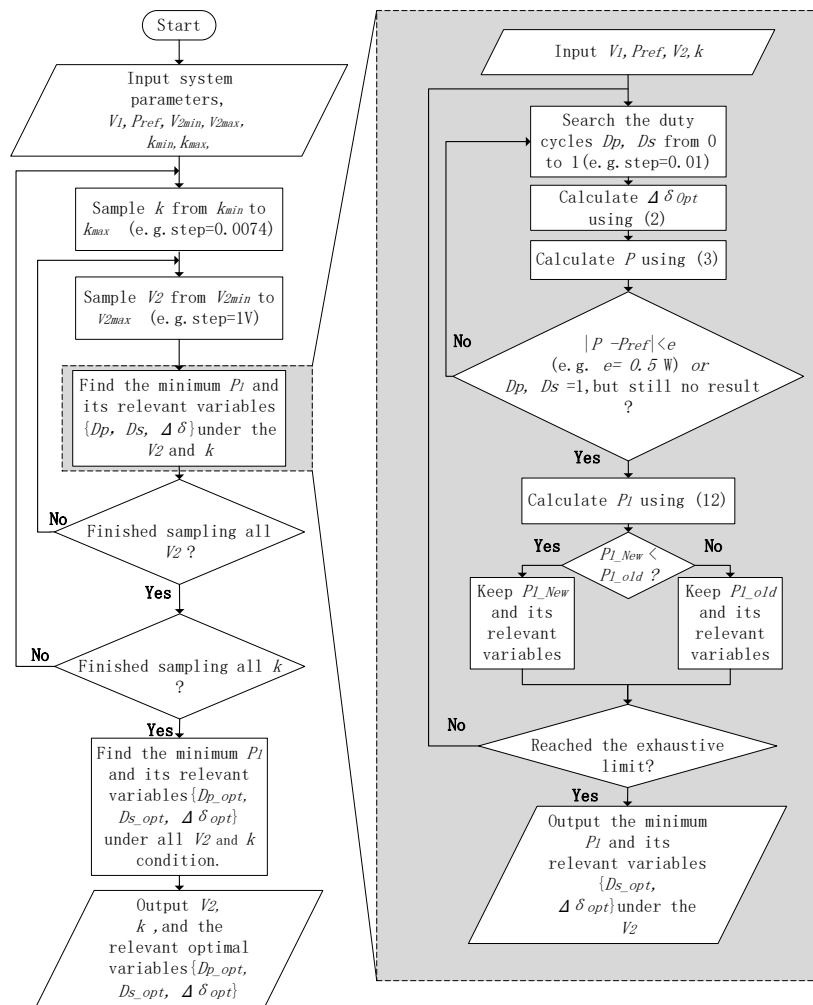


Figure 5. Flowchart for obtaining the optimal variables

### 3. SIMULATION RESULTS AND DISCUSSION

#### 3.1. Specifications

The performance of the proposed wireless charger is validated through simulations conducted in MATLAB/Simulink. The parameters are designed based on the guidelines provided in [1], and all details are shown in Table 1.

#### 3.2. Simulation results under alignment condition

In the simulation, the coupling coefficient is set as 0.302, and the battery voltage is swept from 72 V to 109 V. As shown in Figure 6, the output power generally remains constant within the range of 210 W to 217 W. The system maintains efficiency between 90.72% and 92.46% throughout the entire charging process. The proposed charger delivers competitive efficiency performance when compared with other state-of-the-art

CP wireless charging systems, as detailed in Table 2.

The wireless charger with the proposed control strategy can make sure all of the switches always work in ZVS conditions during the charging process. The waveforms of the inverter output voltage  $u_{ab}$  and the corresponding output current  $I_{L1}$  are presented in Figure 7(a), while Figure 7(b) shows the rectifier input voltage  $u_{cd}$  and input current  $I_{L2}$  under a battery voltage condition of  $V_2 = 109$  V.

Table 1. Parameters of the wireless charger

Variable	Speed (rpm)	Power (kW)
$V_1$	Input DC voltage	73.5 V
$V_2$	Output battery voltage	72 V – 109 V
$k$	Coupling coefficient	0.262 – 0.302
$L_P, L_S$	Transmitting/receiving coil inductance	111 $\mu$ H
$R_{LP}, R_{Ls}$	Transmitting/receiving coil resistance	100 m $\Omega$
$L_1, L_2$	Primary/secondary compensation inductance	35.2 $\mu$ H
$R_{L1}, R_{L2}$	Primary/secondary inductor resistance	100 m $\Omega$
$C_1, C_2$	Primary/secondary parallel capacitance	115 nF
$C_P, C_S$	Primary/secondary series capacitance	53.5 nF
$R_{C1}, R_{C2}$	Primary/secondary parallel capacitance ESR	100 m $\Omega$
$R_{Cp}, R_{Cs}$	Primary/secondary series capacitance ESR	100 m $\Omega$
$R_{ON}$	MOSFET on-state resistance	100 m $\Omega$
$f = \frac{\omega}{2\pi}$	Switching frequency	79 kHz
$I_{ZVS}$	Threshold ZVS current	2 A
$P_{ref}$	Reference power	230 W

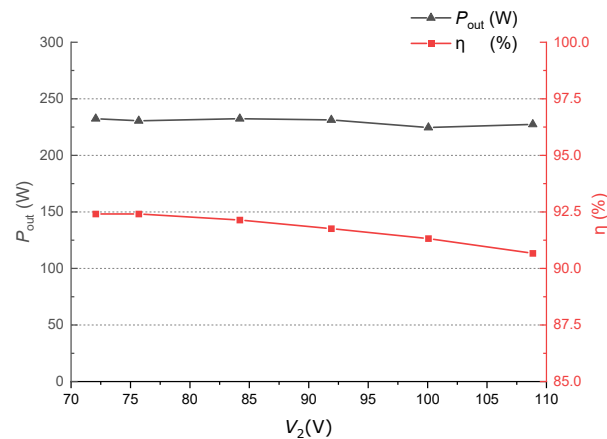


Figure 6. Output power  $P_o$ , and efficiency  $\eta$  versus the different battery voltage  $V_2$  when alignment condition

Table 2. Features comparison between the previous single-stage CP chargers and this work

Different works and published year	2020 [19]	2022 [20]	2022 [22]	2024 [5]	This work
Type of compensation network	S-S	S-S	DS-LCC	LCC-S	DS-LCC
No extra auxiliary SCC	No	Yes	No	Yes	Yes
Efficiency optimization	Yes	Yes	No	Yes	Yes
No large current issue when misalignment	No	No	Yes	Yes	Yes
Bidirectional operation	No	Yes	No	No	Yes
No noticeable current fluctuation	Yes	Yes	Yes	No	Yes
Constant operating frequency	Yes	No	Yes	Yes	Yes
DC to DC efficiency	88.8%	87.9%	91.5%	89.8%	92.46%

### 3.3. Discussion on misalignment condition

To know the performance of the wireless charger under misalignment conditions using the proposed control strategy, a simulation was conducted with the coupling coefficient reduced to 0.262. The output power and efficiency versus battery voltage are illustrated in Figure 8. As observed, the efficiency remains high,

ranging from 91.12% to 92.45%, even under misaligned conditions. The output power is maintained between 190.42 W and 217.56 W. When the output voltage  $V_2$  is in the lower range, a drop in output power is observed. This is attributed to the reduced maximum power transfer capability of the DS-LCC charger at lower coupling coefficients. Nevertheless, the proposed control strategy enables the wireless charger to effectively track the maximum power point while maintaining optimal efficiency. When the coupler is properly designed, the variation of the coupling coefficient  $k$  is typically confined to a narrow range [25]. Therefore, the impact of misalignment on the output power of the wireless charger is relatively limited.

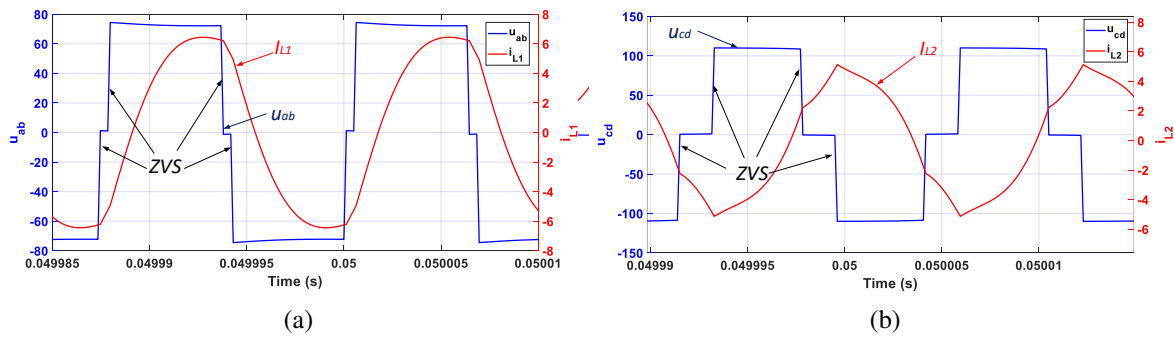


Figure 7. Waveforms of (a) the inverter's output voltage  $u_{ab}$  and current  $i_{L1}$ , (b) the rectifier's input voltage  $u_{cd}$  and current  $i_{L2}$  when  $V_2 = 109 V$

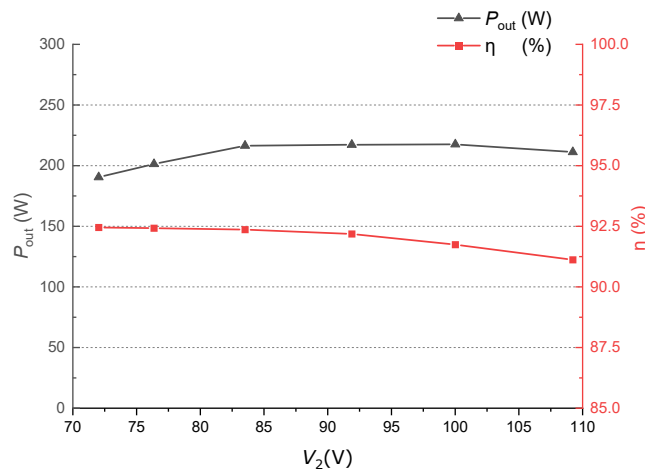


Figure 8. Output current  $I_o$ , and efficiency  $\eta$  versus the different battery voltage  $V_2$  in simulation

#### 4. CONCLUSION

This paper proposed an adaptive constant power optimal efficiency control (ACPOEC) strategy for a bidirectional double-sided LCC (DS-LCC) wireless power transfer charger. The proposed approach integrates triple-phase-shift (TPS) modulation with an offline optimization procedure and a precomputed lookup table to regulate the control variables, enabling constant-power charging while maintaining high efficiency over a wide battery voltage range. In addition, a coupling coefficient estimation method based on current measurement is introduced to allow adaptive control under varying magnetic coupling conditions. By eliminating the need for switch-controlled capacitors, the proposed method simplifies the circuit topology and reduces additional component losses while preserving bidirectional power transfer capability. Simulation results demonstrate that the wireless charger can maintain nearly constant output power throughout the charging process while achieving high efficiency in the range of approximately 90–92%. Furthermore, all switching devices operate under zero-voltage switching conditions, which contributes to reduced switching losses and improved overall

system efficiency. The performance of the proposed strategy was also evaluated under both alignment and misalignment conditions. The results indicate that the system maintains stable power transfer and high efficiency despite variations in the coupling coefficient, demonstrating the robustness of the proposed control scheme. These characteristics make the proposed ACPOEC-based wireless charger a promising solution for practical inductive power transfer applications, particularly in systems requiring efficient, bidirectional, and reliable wireless charging. Future work will focus on hardware implementation and experimental validation to further investigate the practical performance and dynamic behavior of the proposed control strategy.

### FUNDING INFORMATION

The authors sincerely thank the financial support from the Ministry of Higher Education through Universiti Teknologi Malaysia for the High-Tech Research Grant (Vote No. Q.J130000.4623.00Q21) and the Professional Development Research University Grant (Vote No. Q.J130000.21A2.07E30). The authors also gratefully acknowledge the support from the Guangxi Zhuang Autonomous Region Basic Research Capacity Improvement Project for Universities' Young and Middle-aged Teachers (Project No. 2024KY1879).

### AUTHOR CONTRIBUTIONS STATEMENT

This journal uses the Contributor Roles Taxonomy (CRediT) to recognize individual author contributions, reduce authorship disputes, and facilitate collaboration.

Name of Author	C	M	So	Va	Fo	I	R	D	O	E	Vi	Su	P	Fu
Jiabo Yan	✓	✓	✓	✓	✓	✓	✓	✓	✓	✓	✓			
Mohd Junaidi Abdul Aziz		✓				✓	✓			✓		✓	✓	✓
Nik Rumzi Nik Idris		✓				✓	✓			✓		✓	✓	
Mohammad Al Takrouri						✓				✓	✓			
Tole Sutikno						✓	✓			✓		✓		

C : Conceptualization

M : Methodology

So : Software

Va : Validation

Fo : Formal Analysis

I : Investigation

R : Resources

D : Data Curation

O : Writing - Original Draft

E : Writing - Review & Editing

Vi : Visualization

Su : Supervision

P : Project Administration

Fu : Funding Acquisition

### CONFLICT OF INTEREST STATEMENT

The authors declare that they have no known competing financial interests or personal relationships that could have appeared to influence the work reported in this paper.

### DATA AVAILABILITY

The data that support the findings of this study are available from the corresponding author upon reasonable request.

### REFERENCES

- [1] S. Li, W. Li, J. Deng, T. D. Nguyen, and C. C. Mi, "A double-sided LCC compensation network and its tuning method for wireless power transfer," *IEEE Transactions on Vehicular Technology*, vol. 64, no. 6, pp. 2261–2273, 2015, doi: 10.1109/TVT.2014.2347006.
- [2] V. B. Vu, D. H. Tran, and W. Choi, "Implementation of the constant current and constant voltage charge of inductive power transfer systems with the double-sided LCC compensation topology for electric vehicle battery charge applications," *IEEE Transactions on Power Electronics*, vol. 33, no. 9, pp. 7398–7410, 2018, doi: 10.1109/TPEL.2017.2766605.
- [3] R. Tanikawa and H. Le, "Constant power battery charger," WO1996037941A1, 1996, [Online]. Available: <https://patents.google.com/patent/WO1996037941A1>.
- [4] Z. Huang, S. C. Wong, and C. K. Tse, "Design of a single-stage inductive-power-transfer converter for efficient EV battery charging," *IEEE Transactions on Vehicular Technology*, vol. 66, no. 7, pp. 5808–5821, 2017, doi: 10.1109/TVT.2016.2631596.

- [5] I. W. Iam, C. K. Choi, C. S. Lam, P. I. Mak, and R. P. Martins, "A constant-power and optimal-transfer-efficiency wireless inductive power transfer converter for battery charger," *IEEE Transactions on Industrial Electronics*, vol. 71, no. 1, pp. 450–461, 2024, doi: 10.1109/TIE.2023.3241408.
- [6] S. Y. R. Hui and W. C. Ho, "A new generation of universal contactless battery charging platform for portable consumer electronic equipment," *PESC Record - IEEE Annual Power Electronics Specialists Conference*, vol. 1, pp. 638–644, 2004, doi: 10.1109/pesc.2004.1355823.
- [7] L. Zhou, J. Tian, S. Liu, R. Mai, L. Fu, and U. K. Madawala, "High-efficiency WPT systems for potable electronics based on DC-bias-voltage- controlled variable capacitor," *IEEE Transactions on Industrial Electronics*, vol. 71, no. 5, pp. 4707–4718, 2024, doi: 10.1109/TIE.2023.3281675.
- [8] Y. Zhang, S. Chen, X. Li, and Y. Tang, "Design methodology of free-positioning nonoverlapping wireless charging for consumer electronics based on antiparallel windings," *IEEE Transactions on Industrial Electronics*, vol. 69, no. 1, pp. 825–834, 2022, doi: 10.1109/TIE.2020.3048322.
- [9] Q. Chen, S. C. Wong, C. K. Tse, and X. Ruan, "Analysis, design, and control of a transcutaneous power regulator for artificial hearts," *IEEE Transactions on Biomedical Circuits and Systems*, vol. 3, no. 1, pp. 23–31, 2009, doi: 10.1109/TBCAS.2008.2006492.
- [10] A. Aldaoud *et al.*, "Near-field wireless power transfer to stent-based biomedical implants," *IEEE Journal of Electromagnetics, RF and Microwaves in Medicine and Biology*, vol. 2, no. 3, pp. 193–200, 2018, doi: 10.1109/JERM.2018.2833386.
- [11] M. Machnoor and G. Lazzi, "High-efficiency multicoil wireless power and data transfer for biomedical implants and neuroprosthetics," *Antenna and Sensor Technologies in Modern Medical Applications*, 2021, doi: 10.1002/9781119683285.ch8.
- [12] R. Mai, Y. Chen, Y. Zhang, N. Yang, G. Cao, and Z. He, "Optimization of the passive components for an S-LCC topology-based WPT system for charging massive electric bicycles," *IEEE Transactions on Industrial Electronics*, vol. 65, no. 7, pp. 5497–5508, 2018, doi: 10.1109/TIE.2017.2779437.
- [13] A. Triviño-Cabrera, J. M. Gonzalez-Gonzalez, and J. A. Aguado, "Design and implementation of a cost-effective wireless charger for an electric bicycle," *IEEE Access*, vol. 9, pp. 85277–85288, 2021, doi: 10.1109/ACCESS.2021.3084802.
- [14] Z. Bi, T. Kan, C. C. Mi, Y. Zhang, Z. Zhao, and G. A. Keoleian, "A review of wireless power transfer for electric vehicles: prospects to enhance sustainable mobility," *Applied Energy*, vol. 179, pp. 413–425, 2016, doi: 10.1016/j.apenergy.2016.07.003.
- [15] H. Zhang, F. Lu, and C. Mi, "An electric roadway system leveraging dynamic capacitive wireless charging: furthering the continuous charging of electric vehicles," *IEEE Electrification Magazine*, vol. 8, no. 2, pp. 52–60, 2020, doi: 10.1109/MELE.2020.2985486.
- [16] X. Dai, X. Li, Y. Li, and A. P. Hu, "Maximum efficiency tracking for wireless power transfer systems with dynamic coupling coefficient estimation," *IEEE Transactions on Power Electronics*, vol. 33, no. 6, 2018, doi: 10.1109/TPEL.2017.2729083.
- [17] Y. Liu and H. Feng, "Maximum efficiency tracking control method for WPT system based on dynamic coupling coefficient identification and impedance matching network," *IEEE Journal of Emerging and Selected Topics in Power Electronics*, vol. 8, no. 4, pp. 3633–3643, 2020, doi: 10.1109/JESTPE.2019.2935219.
- [18] H. Zhu, B. Zhang, and L. Wu, "Output power stabilization for wireless power transfer system employing primary-side-only control," *IEEE Access*, vol. 8, pp. 63735–63747, 2020, doi: 10.1109/ACCESS.2020.2983465.
- [19] Z. Huang, C. S. Lam, P. I. Mak, R. P. D. S. Martins, S. C. Wong, and C. K. Tse, "A single-stage inductive-power-transfer converter for constant-power and maximum-efficiency battery charging," *IEEE Transactions on Power Electronics*, vol. 35, no. 9, pp. 8973–8984, 2020, doi: 10.1109/TPEL.2020.2969685.
- [20] F. Xu, S. C. Wong, and C. K. Tse, "Overall loss compensation and optimization control in single-stage inductive power transfer converter delivering constant power," *IEEE Transactions on Power Electronics*, vol. 37, no. 1, pp. 1146–1158, 2022, doi: 10.1109/TPEL.2021.3098914.
- [21] China Electricity Council, *GB/T 38775.6-2021: Electric vehicle wireless power transfer - Part 6: Interoperability requirements and testing - Ground side*. China, 2021. [Online]. Available: [https://www.chinesestandard.net/PDF.aspx/GBT38775.6-2021?English\\_GB/T 38775.6-2021](https://www.chinesestandard.net/PDF.aspx/GBT38775.6-2021?English_GB/T%2038775.6-2021).
- [22] Z. Luo, Y. Zhao, M. Xiong, X. Wei, and H. Dai, "A self-tuning LCC/LCC system based on switch-controlled capacitors for constant-power wireless electric vehicle charging," *IEEE Transactions on Industrial Electronics*, vol. 70, no. 1, pp. 709–720, 2023, doi: 10.1109/TIE.2022.3153812.
- [23] X. Zhang *et al.*, "A control strategy for efficiency optimization and wide ZVS operation range in bidirectional inductive power transfer system," *IEEE Transactions on Industrial Electronics*, vol. 66, no. 8, pp. 5958–5969, 2019, doi: 10.1109/TIE.2018.2871794.
- [24] G. Zhu, J. Dong, G. Yu, W. Shi, C. Riekerk, and P. Bauer, "Optimal multivariable control for wide output regulation and full-range efficiency optimization in LCC-LCC compensated wireless power transfer systems," *IEEE Transactions on Power Electronics*, vol. 39, no. 9, pp. 11834–11848, 2024, doi: 10.1109/TPEL.2024.3414157.
- [25] M. Budhia, G. A. Covic, and J. T. Boys, "Design and optimization of circular magnetic structures for lumped inductive power transfer systems," *IEEE Transactions on Power Electronics*, vol. 26, no. 11, pp. 3096–3108, 2011, doi: 10.1109/TPEL.2011.2143730.

## BIOGRAPHIES OF AUTHORS



**Jiabo Yan**     received the M.Sc. degree in transportation engineering from Nanjing University of Aeronautics and Astronautics (NCAA), China, in 2019. He is currently pursuing the Ph.D. degree in electrical engineering with Universiti Teknologi Malaysia (UTM). Since 2022, he has been with the College of Traffic and Transportation, Nanning University, Nanning, China, where he is currently a lecturer. His current research interests include power electronics, electric vehicles, and wireless power transfer. He can be contacted at email: felixyan8051@foxmail.com.



**Mohd Junaidi Abdul Aziz**    was born in Kuala Terengganu, Malaysia, in 1979. He received the B.S. and M.S. degrees in electrical engineering from Universiti Teknologi Malaysia (UTM), Kuala Lumpur, Malaysia, in 2000 and 2002, respectively, and the Ph.D. degree in electrical engineering from the University of Nottingham, Nottingham, England, U.K., in 2008. Since 2008, he has been with the Faculty of Electrical Engineering, UTM, where he is currently an associate professor and head of Power Electronics and Drive Research Group (PEDG). His current research interests include power electronics and electric vehicles, with a special focus on battery management systems. He can be contacted at email: junaidi@utm.my.



**Nik Rumzi Nik Idris**    received the B.Eng. degree in electrical engineering from the University of Wollongong, Australia, in 1989, the M.Sc. degree in power electronics from Bradford University, U.K., in 1993, and the Ph.D. degree from Universiti Teknologi Malaysia (UTM), in 2000. He is currently a professor with the Faculty of Electrical Engineering, UTM, and an associate editor of IEEE Transactions on Power Electronics. Previously, he chaired the IEEE Power Electronics Malaysia Chapter (2014–2016). His research interests include AC drive systems and DSP applications in power electronics. He can be contacted at email: nikrumzi@fke.utm.my.



**Mohammad Al Takroui**    was born in Jeddah, Saudi Arabia, on May 1995. He received a bachelor's degree in electrical engineering from Al-Ahliyya Amman University, Amman. Later in 2020, he obtained his graduate degree in electrical engineering (cum laude) from Politecnico di Milano university, Italy. He is currently working towards his Ph.D. in Universiti Teknologi Malaysia on energy management strategies and control for hybrid energy storage systems. He can be contacted at email: takroui.moh@graduate.utm.my.



**Tole Sutikno**    is a lecturer and the Head of the master's program of Electrical Engineering at the Faculty of Industrial Technology at Universitas Ahmad Dahlan (UAD) in Yogyakarta, Indonesia. He received his Bachelor of Engineering from Universitas Diponegoro in 1999, Master of Engineering from Universitas Gadjah Mada in 2004, and Doctor of Philosophy in Electrical Engineering from Universiti Teknologi Malaysia in 2016. All three degrees are in Electrical Engineering. He has been a Professor at UAD in Yogyakarta, Indonesia, since July 2023, following his tenure as an associate professor in June 2008. He is the Editor-in-Chief of TELKOMNIKA and head of the Embedded Systems and Power Electronics Research Group (ESPERG). He is one of the top 2% of researchers worldwide, according to Stanford University and Elsevier BV's list of the most influential scientists from 2021 to the present. His research interests cover digital design, industrial applications, industrial electronics, industrial informatics, power electronics, motor drives, renewable energy, FPGA applications, embedded systems, artificial intelligence, intelligent control, digital libraries, and information technology. He can be contacted at email: tole@te.uad.ac.id.